

The Fe K α Line and Relativistic Effects from Accretion Disks

Randy R. Ross

Physics Dept., College of the Holy Cross, Worcester, MA 01610, USA

Abstract. One of the most exciting results from *ASCA* has been the discovery of relativistic line profiles for iron K α emission from Seyfert 1 galaxies. Recent results concerning the properties of Fe K α lines from the inner regions of black-hole accretion disks are reviewed.

1. Introduction

Ginga observations showed that Fe K α fluorescence and Compton reflection of X-rays by optically thick matter are common in Seyfert 1 galaxies. The X-ray spectra deviate from simple power laws by exhibiting strong emission features around 6 keV, broad decrements for $7 \lesssim E \lesssim 10$ keV, and steadily rising excesses indicating a flattening of the spectra for $E \gtrsim 10$ keV (e.g., Pounds et al. 1990; Nandra & Pounds 1994—see Mushotzky, Done & Pounds 1993 and references therein). For reflection of hard X-rays, the competition between greater photoabsorption for low-energy photons and greater Compton recoil and penetration depth for high-energy photons produces a peak in the reflected spectrum at around 30 keV (e.g., Lightman & White 1988; George & Fabian 1991). This reflection hump is thought to be responsible for the hard high-energy tail in the total spectrum, while absorption and K α fluorescence by iron produce the decrement above 7 keV and the emission line.

The simplest assumption is that the optically thick material responsible for these reflection and fluorescence features belongs to the putative accretion disk. It should be possible to confirm this by looking for the relativistic effects on the Fe K α line profile produced by the Keplerian motion of the matter and the proximity to the central black hole.

For an X-ray illuminated accretion disk around a Schwarzschild black hole, the expected profiles for fluorescence lines have been calculated by several authors (e.g., Fabian et al. 1989; Stella 1990; Matt et al. 1992; Matt, Fabian & Ross 1993). Figure 1 shows typical line profiles in such a case. The relevant variables are the innermost (r_i) and outermost (r_o) radii of the fluorescing region of the disk, the angle of inclination (i) of the disk, and the radial dependence of the line emissivity, often taken to be proportional to r^{-q} for simplicity. The profiles in Fig. 1 have been calculated assuming $q = 2$, so that all included portions of the disk make important contributions to the total line flux. These particular profiles are only approximate, since they have been calculated treating relativistic effects to lowest order as described by Chen, Halpern & Filippenko (1989).

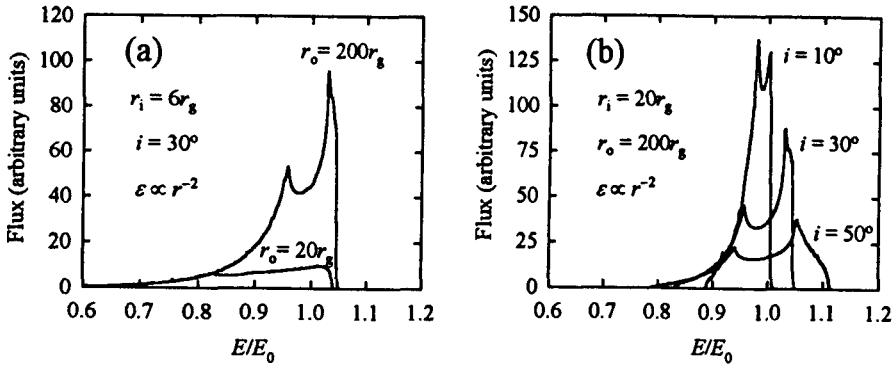


Figure 1. Calculated accretion-disk line profiles assuming an emissivity proportional to r^{-2} . E is the observed photon energy, while E_0 is the line energy in the rest frame of the emitting plasma. (a) Profiles for an inner radius of $6r_g$ and an inclination of 30° assuming that the fluorescing region extends all the way to $200r_g$ (upper curve) or only to $20r_g$ (lower curve). (b) Profiles for $20r_g < r < 200r_g$ with inclination angles of 10° , 30° , or 50° as indicated.

Fig. 1(a) shows the line profile when $i = 30^\circ$ and the fluorescing region extends from the innermost stable orbit at $6r_g$ (where $r_g = GM/c^2$ is the gravitational radius of the black hole) all the way to $200r_g$. For the approaching portion of the disk surface, competition between the Doppler blueshift and the gravitational and transverse-Doppler redshifts results in a narrow blue peak or “horn” with a steep wing. For the receding portion of the surface, however, the Doppler and gravitational redshifts reinforce each other, resulting in a broad red wing with a lower peak. Unless the inclination is high, line emission from the innermost portion of the disk is strongly redshifted. For example, Fig. 1(a) shows the contribution to the line profile due solely to the region $6r_g < r < 20r_g$. Nearly all of this emission is redshifted, and this region is entirely responsible for the farthest red wing of the “full” profile.

The effects of inclination are shown in Fig. 1(b). At low inclination, the gravitational and transverse-Doppler redshifts dominate, so that the emission is mostly redshifted. At higher inclination, the radial Doppler effect increases in importance, so that the “horns” of the line profile become more widely separated, and the far line wings fall off less steeply.

Line profiles for an accretion disk around a Kerr black hole have been calculated by Laor (1991) and Kojima (1991). The most important differences result from the fact that the disk can extend to smaller radii, since the innermost stable orbit is at $r_i \approx 1.24r_g$ for a black hole rotating with maximum possible angular momentum (Thorne 1974). As a result, the far red wing of the line is enhanced at low inclination, while at high inclination the blue “horn” is especially enhanced by Doppler beaming.

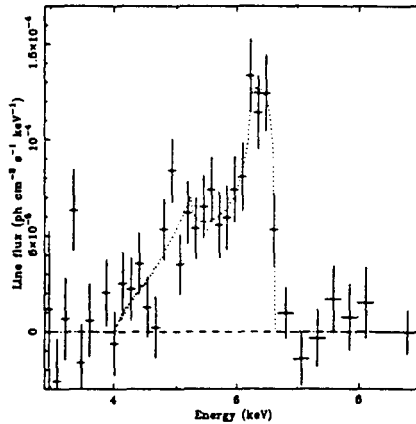


Figure 2. Observed Fe $K\alpha$ line profile for MCG-6-30-15. Data points show the deviation from the best-fit model for the continuum, taking into account the response of the detector. The *ASCA* SIS data have been rebinned to approximately the instrumental resolution. The dotted curve shows the best-fit line profile for an illuminated accretion disk around a Schwarzschild black hole. (From Tanaka et al. 1995)

2. Fe $K\alpha$ Profiles Observed by *ASCA* for Seyfert Galaxies

Although the spectral resolution of *Ginga* was too low ($\Delta E/E \sim 18\%$) to allow detailed study of Fe $K\alpha$ line profiles, some evidence of broad ($\sigma \sim 0.9$ keV) lines was found for Seyfert 1s (e.g., Pounds et al. 1989; Nandra & Pounds 1994). The higher spectral resolution of *ASCA* ($\Delta E/E \sim 2\%$ at 6 keV for the Solid-state Imaging Spectrometer) has made it possible to study the line profiles in much greater detail.

2.1. The Line Profile for MCG-6-30-15

Tanaka et al. (1995) found a broad, skewed line profile in an *ASCA* observation of the Seyfert 1 galaxy MCG-6-30-15. The observation was especially long (4.2 d), yielding good signal-to-noise ratios. The observed Fe $K\alpha$ line profile is shown in Figure 2. The line shape is highly asymmetric, with a narrow peak around 6.4 keV and a broad red wing extending to 4–5 keV. The full width at zero intensity implies velocities $\sim 100,000$ km s $^{-1}$. Fitting the data with the line profile for an accretion disk in the Schwarzschild metric gives an inclination $i \sim 30^\circ$, a fluorescing region covering $6r_g \lesssim r \lesssim 20r_g$, an emission-law parameter $q \sim 1-3$, and an equivalent width $EW \sim 300-400$ eV.

An explanation for the observed emission feature other than a relativistic accretion disk appears unlikely. The broad profile cannot be due to a blend of lines, since most of the emission occurs at energies below that of the Fe I line in the rest frame of the galaxy. The broad red wing cannot be due to Compton scattering of the line photons as they escape from the fluorescing gas, since this only produces a red shoulder two Thomson wavelengths ($\Delta E \approx 0.16$ keV)

wide (Basko 1978). Similarly, the red wing cannot be due to Comptonization by transmission through a plasma. To produce such broadening and reddening would require an optical depth $\tau_T \sim 5$ of cold gas. This would produce a Compton cutoff in the spectrum,

$$E_{\text{cutoff}} \approx \frac{m_e c^2}{\tau_T^2} \sim 20 \text{ keV},$$

whereas observations reveal that the spectrum does not cut off until ~ 600 keV (Zdziarski et al. 1995). Fabian et al. (1995) have argued that attempting to explain the line profile via Doppler shifts from outflows presents various problems, such as inconsistency with the low velocity of the warm absorber implied by the observed energy of the O VII K-edge. The Fe K α line appears to be showing the signature of matter in orbit very close to the central black hole.

Recently Iwasawa et al. (1996a) have studied the variability of the iron line during the 4.2-d observation of MCG-6-30-15. For much of the analysis, the line profile was modeled with two gaussian components—a narrow one ($\sigma_N = 0.15$ keV) centered at $E_N = 6.4$ keV representing the line core and a broad one ($\sigma_B = 0.64$ keV) centered at $E_B = 5.5$ keV representing the red wing. These components roughly represent the emission from portions of the disk at greater and lesser distances, respectively, from the black hole. The two components were found to vary in different ways over different time scales.

Over two extended periods (~ 1.5 d and ~ 2.0 d) of “intermediate” total flux, continuum changes on short time scales ($\Delta t \sim 10^3$ – 10^4 s) were accompanied by a correlated behavior in the intensity of the broad component, while the intensity of the narrow component remained nearly constant. In a simple illumination model, the line intensity would be expected to follow the continuum flux. Apparently rapid changes in the continuum are produced by brief flares occurring at small radii (where relevant time scales are the shortest), so that only the broad, highly redshifted component of the K α line responds to them.

Over an extended period (2.5×10^4 s) when the total flux was in a deep minimum, however, there was no significant detection of the narrow line, while the red wing was actually somewhat stronger than during the periods of intermediate total flux. The observed line profile for this period is shown in Figure 3. Here the red wing extends to such low energies that it cannot be modeled adequately by an accretion-disk line in Schwarzschild geometry. Kerr geometry must be assumed to get the best fit, with an inclination $i \sim 30^\circ$, a fluorescing region covering $1.24 r_g \lesssim r \lesssim 16 r_g$, and an emissivity $\epsilon \propto r^{-3}$, so that the innermost regions dominate the line emission. The equivalent width is then $EW \sim 1.3$ keV.

While the possible evidence for rotation of the central black hole is intriguing, the large equivalent width found for the iron line is problematic. The expected EW for fluorescence of cold iron is only ~ 100 – 200 eV (e.g., George & Fabian 1991). Several factors could be involved in increasing the observed equivalent width. First, iron could be overabundant compared to solar values. Second, for a rapidly spinning black hole, considerable radiation from small radii of the disk would be expected to return to the disk surface by light bending (Cunningham 1976), enhancing the equivalent width. Finally, the inner disk could be highly ionized by the illuminating radiation. Photoionization/recombination of

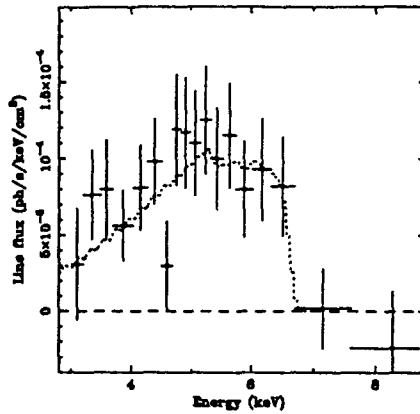


Figure 3. Line profile for MCG-6-30-15 observed during a deep minimum in the total X-ray flux. The dotted curve shows the best-fit line profile for an illuminated accretion disk assuming that the central black hole is rotating with maximum possible angular momentum. (From Iwasawa et al. 1996a)

Fe xxv produces a larger EW than fluorescence of less highly ionized iron (see Matt et al. 1993; Życki & Czerny 1994).

Near the middle of the observation of MCG-6-30-15, there was an extended period ($\sim 3 \times 10^4$ s) of especially high total flux. During this time the line profile was dominated by the narrow core around 6.4 keV, while the red wing was somewhat suppressed. Iwasawa et al. (1996a) speculated that activity during this interval may have been dominated by a large flare above the approaching side of the disk (at say $r \sim 7r_g$) so that it contributed little to the red wing of the line profile. *Note:* the assumption that only a few flares take place above the disk at any given time is consistent with the rapid variability of the total flux (Reynolds et al. 1995) and recent theoretical work implying that the accretion-disk corona must consist of individual blobs (e.g., Haardt, Maraschi & Ghisellini 1994; Stern et al. 1995).

2.2. Line Profiles for Other Seyfert Galaxies

ASCA observations have revealed skewed Fe $K\alpha$ lines with broad red wings for the Seyfert galaxies Fairall 9 (Otani et al. 1996), NGC 4151 (Yaqoob et al. 1995), and IRAS 18325-5926 (Iwasawa et al. 1996b—here the broad iron line and rapid variability of the continuum are unusual for the source's classification as a Seyfert 2.) Broad, redshifted lines (with signal-to-noise ratios too poor to reveal detailed line shapes) were also found for NGC 5548 and IC 4329A (Mushotzky et al. 1995) as well as NGC 4051 (Guainazzi et al. 1996).

Recently Nandra et al. (1996) have reported the results of observing 18 Seyfert 1 galaxies with *ASCA*. They found that 14 of the sources showed an iron $K\alpha$ line which was resolved, with a mean width $\langle \sigma \rangle = 0.43 \pm 0.12$ keV for a gaussian profile. Furthermore, many of the line profiles were asymmetric

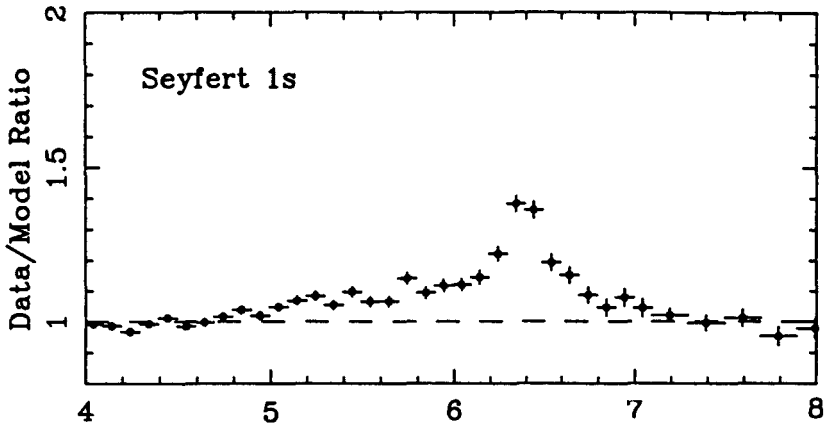


Figure 4. Composite Fe $K\alpha$ line profile resulting from *ASCA* observations of 18 Seyfert 1 galaxies. The abscissa is the photon energy in keV. The model used in obtaining the data/model ratio for each source is the best power law fit to the 3–10 keV SIS data excluding the 5–7 keV iron band. (From Nandra et al. 1996)

with broad red wings. A composite line profile for all 18 sources is shown in Figure 4. The characteristic features of a line from a low-inclination accretion disk are apparent: the narrow core around 6.4 keV, the steep drop-off toward higher energies, and the broad red wing extending down to ~ 5 keV. Disk-line fits to the data for the individual sources yield a mean inclination $\langle i \rangle = 29^\circ \pm 3^\circ$ and a mean value of the emission-law parameter $\langle q \rangle = 2.5 \pm 0.4$. Differences in the values of q (with r_i and r_o fixed in the analysis) imply that the line emission geometry does vary from source to source. Although the average emissivity function implies that $\sim 50\%$ of the line emission originates within $r \lesssim 20r_g$, Nandra et al. (1996) found no compelling evidence for preferring the closer-reaching disk around a Kerr black hole over a disk in the Schwarzschild metric. The mean value for the equivalent width of the line is 230 ± 60 eV when a Compton reflection component is included in the model for the continuum. Therefore, many of these AGNs only need to be moderately metal-rich to account for the observed EW of the Fe $K\alpha$ line.

The iron lines for most Seyfert 2 galaxies do *not* reveal the characteristics of emission by an accretion disk. This is in keeping with the unification scheme for AGNs (Antonucci 1993), in which the accretion disk of a Seyfert 2 galaxy is obscured by the molecular torus. For example, the archetypal Seyfert 2 galaxy NGC 1068 shows a blend of three *narrow* Fe lines (Ueno et al. 1994—also see Marshall et al. 1993): near-neutral iron (~ 6.4 keV) with $EW = 1.6 \pm 0.4$ keV, Fe XXV (~ 6.7 keV) with $EW = 1.0 \pm 0.45$ keV, and Fe XXVI (~ 7.0 keV) with $EW = 0.6 \pm 0.35$ keV. The line at 6.4 keV probably comes from the molecular torus, which is expected to produce a narrow line with $EW \sim 1$ –2 keV (Ghisellini, Haardt & Matt 1994; Matt, Brandt & Fabian 1996). The narrow Fe XXV and Fe XXVI lines are probably produced in the warm scattering region, where

emission via recombination and fluorescence are enhanced by resonant scattering of the X-ray continuum (see Krolik & Kallman 1987; Band et al. 1990; Krolik & Kriss 1995; Matt et al. 1996).

2.3. Discussion

The Fe $K\alpha$ line profiles for a number of Seyfert 1 galaxies have been found to exhibit the features expected from a relativistic accretion disk. Disk-line fits to the data generally imply low inclinations ($i \sim 30^\circ$), whereas random orientations would produce a mean inclination $\langle i \rangle = 60^\circ$. This is in keeping with the unification scheme, in which an AGN must be viewed at low inclination to prevent the molecular torus from obscuring the broad line region and, along with it, the accretion disk. By analyzing the detailed line shapes and their time variability, we can hope to learn much about the geometry of the fluorescing accretion-disk gas and even the rotational state of the central black hole. It should be noted, however, that several factors add to the difficulty of such an analysis.

The modeling of the X-ray continuum can affect the deduced line profile. Both reflection by the accretion disk and transmission through the surrounding “warm absorber” introduce an iron K-edge into the total spectrum that can become confused with the steep blue tail of the emission line. This can result in an underestimation of the line emission as well as an overestimation, depending on how the continuum is treated. For example, Cappi et al. (1996) found a model for the *ASCA* data of IC 4329A that implied a weak, narrow line by letting the reflected component have an amplitude ~ 3 times greater than the direct component, thereby modeling much of the excess emission above 5 keV as part of the hard reflection tail. The assumed reflection component should be consistent with the overall geometry of the disk illumination. Furthermore, the treatment of the iron K-edge in the reflection component should include the “smearing” produced by the gravitational redshift and Doppler effect, just as for the emission line (see Ross, Fabian & Brandt 1996).

The geometry of the primary X-ray emission, and hence the disk illumination, is probably both complicated and variable. As mentioned previously, the primary emission may occur in localized flares above the accretion disk. In most of the disk-line fits to *ASCA* data, the spatial dependence of the line emissivity has been assumed to be $\varepsilon \propto r^{-q}$. Then the variables representing the geometry of the emission are the parameter q and the boundaries (r_i and r_o) of the fluorescing region. This is a convenient way to construct models, but it may not be a very accurate representation of the actual emission region(s).

Finally, part of the Fe $K\alpha$ emission from Seyfert 1 galaxies may originate in regions other than the accretion disk. In this case, the molecular torus can contribute $\Delta EW < 100$ eV in the form of a narrow 6.4-keV line (Ghisellini et al. 1994; Krolik, Madau & Życki 1994). Highly ionized iron in the warm scattering region can also contribute to the total line emission (Krolik & Kallman 1987). Thus the Fe $K\alpha$ line profile may be telling us about more than just the accretion disk.

3. The Spectra of Galactic Black Hole Candidates

The X-ray spectra of galactic black hole candidates (BHCs) also exhibit features due to reflection and fluorescence. Above 6 keV, *EXOSAT* and *Ginga* spectra of BHCs (e.g., Tanaka 1991; Ebisawa 1991; Done et al. 1992) are similar to those of Seyfert 1 galaxies with two important differences. First, the Fe $K\alpha$ line is weaker, with $EW \sim 60$ eV. Second, the decrement (compared to a simple power-law spectrum) above 7 keV is stronger and broader, extending to ~ 20 keV.

BBXRT observations of Cyg X-1 (Marshall et al. 1993) and LMC X-1 (Schlegel et al. 1994) showed little evidence of line emission. Recently, Ebisawa et al. (1996) have analyzed *ASCA* observations of Cyg X-1. A relatively narrow ($\sigma < 0.20$ keV) iron line was detected at 6.4 keV with $EW \sim 10\text{--}40$ eV, although the data did not rule out a broad line with $EW < 100$ eV.

The accretion process in BHCs is probably similar to that in AGNs, so why are the reflection and fluorescence features found to be different? The answer may lie in the high ionization state of the accretion disk. For a “bare” (unilluminated) accretion disk, the effective temperature varies as $T_{\text{eff}} \propto m^{-1/4}$ for given values of r/r_g and the accretion rate as a fraction of the Eddington limit (Shakura & Sunyaev 1973). For an AGN disk, the matter is cold and not highly ionized unless the illumination by the primary X-rays is very strong. For a BHC, with central mass m smaller by a factor of a million or more, the normal temperature of the disk is much higher. Collisions and disk radiation then keep the matter highly ionized, regardless of the amount of X-ray illumination.

This can lead to suppression of the Fe $K\alpha$ line and enhancement of the K-absorption feature. For Fe xvii–xxii, a photon produced by the $1s^2 2s^2 2p^n \rightarrow 1s^2 2s^2 2p^{n-1}$ transition following K-shell photoionization is subject to resonant trapping. Resonant absorption followed by autoionization destroys much of the $K\alpha$ radiation (see Ross & Fabian 1993; Życki & Czerny 1994). Since the elements lighter than iron are fully ionized, the albedo of the disk is high for energies below the iron K-edge. This makes the iron edge more prominent in the total (direct + reflected) spectrum. The strong absorption profile is smeared out by Doppler blurring, gravitational redshift, and the transverse Doppler effect (Ross, Fabian & Brandt 1996).

The weakness of the Fe $K\alpha$ line in BHCs makes it more difficult to observe any relativistic effects from the accretion disk. For LMC X-1, Schlegel et al. (1994) reported the possible detection of two small, narrow emission features at ~ 5.1 and ~ 7.3 keV, each with $EW \sim 60$ eV, which could be the “horns” of the line profile for an accretion disk at high inclination ($i \sim 70^\circ$). Recently Tanaka (1996) has made a stronger claim for GRS 1009–45, which is identified as a BHC because of its ultrasoft spectrum accompanied by a hard power-law tail. An *ASCA* observation revealed a fairly broad emission feature with a (*blueshifted*) peak near 7.2 keV. Assuming that the emission is by Fe xxv ($E_0 = 6.7$ keV), the line shape is fit by a disk-line profile corresponding to a moderate inclination ($i \sim 40^\circ$).

Since galactic black hole candidates lack the obscuring tori of active galactic nuclei, a broader range of inclinations can be expected to be found for these sources. With their weaker Fe $K\alpha$ lines, however, it remains to be seen if BHCs

will reveal as much information about their accretion processes as Seyfert 1 galaxies.

Acknowledgments. Many thanks to my collaborators—Andy Fabian, Giorgio Matt, and Niel Brandt.

References

- Antonucci, R. 1993, *ARA&A*, 31, 473
- Band, D. L., Klein, R. I., Castor, J. I., & Nash, J. K. 1990, *ApJ*, 362, 90
- Basko, M. M., 1978 *ApJ*, 223, 268
- Cappi, M., Mihara, T., Matsuoka, M., Hayashida, K., Weaver, K. A., & Otani, C. 1996, *ApJ*, 458, 149
- Chen, K., Halpern, J. P., & Filippenko, A. V. 1989, *ApJ*, 339, 742
- Cunningham, C. 1976, *ApJ*, 208, 534
- Done, C., Mulchaey, J. S., Mushotzky, R. F., & Arnaud, K. A. 1992, *ApJ*, 395, 275
- Ebisawa, K. 1991, Ph.D. thesis, University of Tokyo
- Ebisawa, K., Ueda, Y., Inoue, H., Tanaka, Y., White, N. E. 1996, *ApJ*, 467, 419
- Fabian, A. C., Nandra, K., Reynolds, C. S., Brandt, W. N., Otani, C., Tanaka, Y., Inoue, H., & Iwasawa, K. 1995, *MNRAS*, 277, L11
- Fabian, A. C., Rees, M. J., Stella, L., & White, N. E. 1989, *MNRAS*, 238, 729
- George, I. M., & Fabian, A. C. 1991, *MNRAS*, 249, 352
- Ghisellini, G., Haardt, F., & Matt, G. 1994, *MNRAS*, 267, 743
- Guainazzi, M., Mihara, T., Otani, C., & Matsuoka, M. 1996, in *MPE Report 263, Röntgenstrahlung from the Universe*, H. U. Zimmermann, J. E. Trümper & H. Yorke, Garching: Max-Planck-Institut für Extraterrestrische Physik, 451
- Haardt, F., Maraschi, L., & Ghisellini, G. 1994, *ApJ*, 432, L95
- Iwasawa, K., et al. 1996a, *MNRAS*, in press
- Iwasawa, K., Fabian, A. C., Mushotzky, R. F., Brandt, W. N., Awaki, H., & Kunieda, H. 1996b, *MNRAS*, 279, 837
- Kojima, Y. 1991, *MNRAS*, 250, 629
- Krolik, J. H., & Kallman, T. R. 1987, *ApJ*, 320, L5
- Krolik, J. H. & Kriss, G. A. 1995, *ApJ*, 447, 512
- Krolik, J. H., Madau, P., & Życki, P. T. 1994, *ApJ*, 420, L57
- Laor, A. 1991, *ApJ*, 376, 90
- Lightman, A. P., & White, T. R. 1988, *ApJ*, 335, 57
- Marshall, F. E., et al. 1993, *ApJ*, 405, 168
- Marshall, F. E., Mushotzky, R. F., Petre, R., & Serlemitsos, P. J. 1993, *ApJ*, 419, 301
- Matt, G., Brandt, W. N., & Fabian, A. C. 1996, *MNRAS*, 280, 823
- Matt, G., Fabian, A. C., & Ross, R. R. 1993, *MNRAS*, 262, 179

- Matt, G., Perola, G. C., Piro, L., & Stella, L. 1992, *A&A*, 257, 63 (erratum 263, 453)
- Mushotzky, R. F., Done, C., & Pounds, K. A. 1993, *ARA&A*, 31, 717
- Mushotzky, R. F., Fabian, A. C., Iwasawa, K., Kunieda, H., Matsuoka, M., Nandra, K., & Tanaka, Y. 1995, *MNRAS*, 272, L9
- Nandra, K., George, I. M., Mushotzky, R. F., Turner, T. J., & Yaqoob, T. 1996, *ApJ*, in press
- Nandra, K., & Pounds, K. A. 1994, *MNRAS*, 268, 405
- Otani, C., et al. 1996, in MPE Report 263, *Röntgenstrahlung from the Universe*, H. U. Zimmermann, J. E. Trümper & H. Yorke, Garching: Max-Planck-Institut für Extraterrestrische Physik, 495
- Pounds, K. A., Nandra, K., Stewart, G. C., George, I. M., & Fabian, A. C. 1990, *Nat*, 344, 132
- Pounds, K. A., Nandra, K., Stewart, G. C., & Leighly, K. 1989, *MNRAS*, 240, 769
- Reynolds, C. S., Fabian, A. C., Nandra, K., Inoue, H., Kunieda, H., & Iwasawa, K. 1995, *MNRAS*, 277, 901
- Ross, R. R., & Fabian, A. C. 1993, *MNRAS*, 261, 74
- Ross, R. R., Fabian, A. C., & Brandt, W. N. 1996, *MNRAS*, 278, 1082
- Schlegel, E. M., Marshall, F. E., Mushotzky, R. F., Smale, A. P., Weaver, K. A., Serlemitsos, P. J., Petre, R., & Jahoda, K. M. 1994, *ApJ*, 422, 243
- Shakura, N. I., & Sunyaev, R. A. 1973, *A&A*, 24, 337
- Stella, L. 1990, *Nat*, 344, 747
- Stern, B. E., Poutanen, J., Svensson, R., Sikora, M., & Begelman, M. C. 1995, *ApJ*, 449, L13
- Tanaka, Y. 1991, in *Lecture Notes in Physics 385, Iron Line Diagnostics in X-ray Sources*, A. Treves, G. C. Perola & L. Stella, Berlin: Springer, 98
- Tanaka, Y. 1996, in MPE Report 263, *Röntgenstrahlung from the Universe*, H. U. Zimmermann, J. E. Trümper & H. Yorke, Garching: Max-Planck-Institut für Extraterrestrische Physik, 85
- Tanaka, Y., et al. 1995, *Nat*, 375, 659
- Thorne, K. S. 1974, *ApJ*, 191, 507
- Ueno, S., Mushotzky, R. F., Koyama, K., Iwasawa, K., Awaki, H., & Hayashi, I. 1994, *PASJ*, 46, L71
- Yaqoob, T., Edelson, R., Weaver, K. A., Warwick, R. S., Mushotzky, R. F., Serlemitsos, & P. J., Holt, S. S. 1995, *ApJ*, 453, L81
- Zdziarski, A. A., Johnson, W. N., Done, C., Smith, D., & McNaron-Brown, K. 1995, *ApJ*, 438, L63
- Życki, P. T., & Czerny, B. 1994, *MNRAS*, 266, 653

Discussion

A. King: It is important to remember that the Boyer-Lindquist radial coordinate r is a very poor measure of proper distance, particularly for Kerr geometries with $a \sim M$. This must affect the emissivity if written as a function of r .

R. Ross: Yes, this is another reason why $\varepsilon \propto r^{-q}$ is likely to be an oversimplification of the fluorescent-line emissivity.

M. Nowak: Are you worried that such a simple model (reflection from a cold, flat disk from a very narrow range, very close to the central hole) seems to work so well? Why isn't it more complicated?

R. Ross: Perhaps such a narrow range of radii works so well because the primary emission is produced by a small number of flares above the disk.

M. Nowak: For the reflection model of Cyg X-1, you also expect roughly $\sim 40\%$ of the total luminosity in a soft (~ 300 eV) component. This is not seen. (Ionisation can hide the Fe-line, it can't hide the soft continuum). Can we really use a reflection model for this source (or any low-state galactic Black Hole candidate)?

R. Ross: This is a genuine concern, but how else could the strong, broad decrement above 7 keV be produced?